Chin. J. Astron. Astrophys. Vol. 5 (2005), No. 2, 144–150
(*http://www.chjaa.org*)

Chinese Journal of
Astronomy and
Astrophysics

$C^{18}O$ Observations of the Dark Molecular Cloud L134 and Gas Depletion onto Dust *

Xin-Jie Mao and Xiao-Xia Sun

Department of Astronomy, Beijing Normal University, Beijing 100875; *maoxj@bnu.edu.cn*

Received 2004 August 25; accepted 2005 February 5

Abstract We map the dark molecular cloud core of L134 in the $C^{18}O$ ($J = 1-0$) emission line using the PMO 13.7 m telescope, and present a contour map of integrated intensity of $C^{18}O$ ($J = 1-0$) emission. The $C^{18}O$ cloud is inside the distribution of extinction A_B, the visual extinction of blue light, as well as inside the ^{13}CO cloud in the L134 region. The depletion factors in this $C^{18}O$ cloud are generally greater than unity, which means there is gas depletion onto dust. Since only a minimum $A_B = 9.7$ mag is available, and our observations measure both undepleted and depleted regions along the line of sight, the depletion factors could very likely be larger in the central core than the calculated value. So we conclude that depletion does occur in the bulk of the $C^{18}O$ cloud through a comparison between the $C^{18}O$ and blue extinction maps in the L134 region. There is no direct evidence as yet for star formation in L134, and so cores on the verge of collapse will not be visible in CO and other gas molecules.

Key words: ISM: clouds – ISM: individual (L134) – ISM: molecules – ISM: extinction

1 INTRODUCTION

L134 is a small and very opaque dark cloud, situated at an unusually high galactic latitude, $b = 35.7°$, and approximately in the direction of the galactic center, $l = 4.2$. The distance of L134 has been estimated to be 100±50 pc from optical observations (Mattila 1979). Since L134 is a high galactic latitude dark cloud, it is relatively isolated in the sky and thus largely uncluttered by material along the line of sight. Moreover, the lack of internal stellar energy sources, with no star formation activities and simple geometric shape have made L134 a good sample to study physical properties and molecular processes in dark molecular clouds both observationally and theoretically.

The size of the dark cloud core of L134 depends on the tracers used for the mapping. For example, the OH cloud is $10' \times 26'$ (Mattila et al. 1979), while the ^{13}CO cloud is $30' \times 40'$ (Minn

* Supported by the National Natural Science Foundation of China (No. 10273002).

et al. 1996). Several other molecules as well as neutral hydrogen have been observed in L134. Some mapping work has been carried out, e.g., for H_2CO by Brook et al. (1976), for CO by Mahoney et al. (1976), and for HI by van der Werf et al. (1988). In addition the molecules CH, CS, HCN, HCO^+, HNC, NH_3, DNC, and DCO^+ have been observed in one or more positions in L134. The extinction in the central area of L134 is $A_B \geq 9.7$ mag. The observations of OH and H_2CO molecules, and of neutral hydrogen HI indicate the cloud of L134 is rotating, but the ^{13}CO observations by Minn et al. (1996) gave no apparent evidence of rotation. It is evident from recent studies of dark clouds that gas depletion leads to a decrease of the component of gas phase, which strongly affects the physical and chemical properties of the clouds. The disappearance of major gas coolants, such as CO, may affect the thermal balance of dark clouds (Goldsmith & Langer 1978). Also CO is widely used to determine the distribution of molecular hydrogen in the interstellar medium, and therefore a number of physical parameters such as the H_2 volume density, the mass distribution, and the cloud mass will be underestimated if a significant amount of CO molecules is stuck on dust grains. Consequently, it is clear that understanding the physical processes in interstellar clouds requires the knowledge of the gas phase depletion. To reveal the $C^{18}O$ depletion onto dust, we compare the distribution of the integrated intensities of $C^{18}O$ emission lines with extinction maps. In Sect. 2 our $C^{18}O$ observations are presented. The $C^{18}O$ map and a comparison with others are given in Sect. 3. In Sect. 4 we discuss the gas depletion onto dust and give a brief conclusion.

2 OBSERVATIONS

In January 2002, observations of the $J = 1 - 0$ transition of $C^{18}O$ were carried out with the 13.7 m antenna at the Qinghai station of Purple Mountain Observatory in Qinghai Province. The half-power beam width of the telescope was about $60''$ at the frequency of 109.78 GHz emitted by the transition of $J = 1 - 0$ in $C^{18}O$. The pointing accuracy was better than $10''$. A 3 mm SIS receiver was used as a front-end with a single-sideband system noise temperature ($T_{\rm sys}$) about 250 K. The backend was a 1024 channel acousto-optical spectrometer with a total band width of 168.6 MHz, a channel spacing of 164.65 kHz (corresponding to a velocity spacing of ~ 0.45 km s^{-1} at 109.8 GHz), and a frequency resolution of 250 kHz (velocity resolution of ~ 0.68 km s^{-1} at 109.8 GHz). The radiation temperature can be obtained from the equation $T_R^* = T_{\rm A}^*/\eta_{\rm fss}$, where $T_{\rm A}^*$ is the antenna temperature corrected for atmospheric attenuation, resistive losses, rearward spillover and scattering, and $\eta_{\rm fss}$ ($\eta_{\rm fss} = 0.61$ at 110 GHz) is the forward spillover and scattering efficiency. The system rms noise level at the spectrum resolution of 0.68 km s^{-1} was on the average a bit more than 0.2 K (for an integration time of 120 seconds). Observations were done in a position-switching mode with a reference point located $4'$ north of the origin of the mapping grid, but its right ascension remained the same as the mapping grid origin, at $\alpha = 15^{\rm h}51^{\rm m}00^{\rm s}$, $\delta = -4^\circ\ 30'\ 00''$ (1950). We have observed a region of $13' \times 25'$ with a grid spacing of $1'$, and the integration time for each spot was 2 min. In addition, in order to measure the relative error of the antenna temperatures, we implemented observations at the position $\alpha = 15^{\rm h}51^{\rm m}00^{\rm s}$, $\delta = -4^\circ\ 26'57''$ (1950) (namely ($0.0'$, $0.0'$), see Sect.2) of L134 at various elevation and horizontal angles. The averaged $T_{\rm A}^*$ is then 1.44 ± 0.23 K, inducing a relative error of 0.16.

3 OBSERVATIONAL RESULTS

We notice that $C^{18}O$ ($J = 1 - 0$) lines obtained during the observing session generally have a higher level of rms, e.g., in the line shown in Fig. 1 at the position ($0.0'$, $0.0'$), corresponding to $\alpha = 15^{h}51^{m}00^{s}$, $\delta = -4^{\circ}\ 26'57''$ (1950), of the $C^{18}O$ map in Fig. 2, which was very likely caused by the degenerated acousto-optical spectrometer.

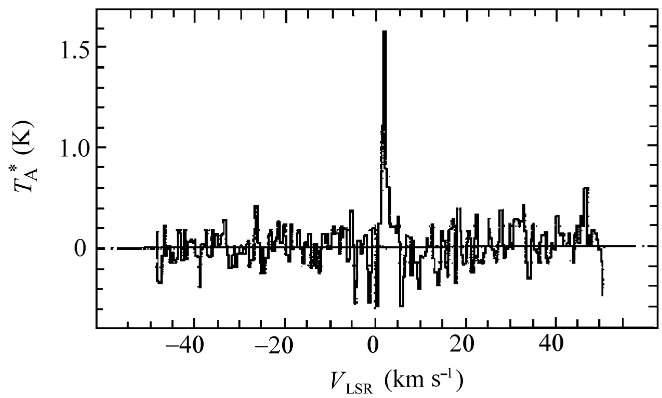

Fig. 1 $C^{18}O$ ($J = 1 - 0$) emission line at the position (0.0′, 0.0′) in the $C^{18}O$ map for the dark molecular cloud core of L134. The coordinates of position (0.0′, 0.0′) are $\alpha = 15^{h}51^{m}00^{s}$, $\delta = -4^{\circ}\ 26'57''$ (1950).

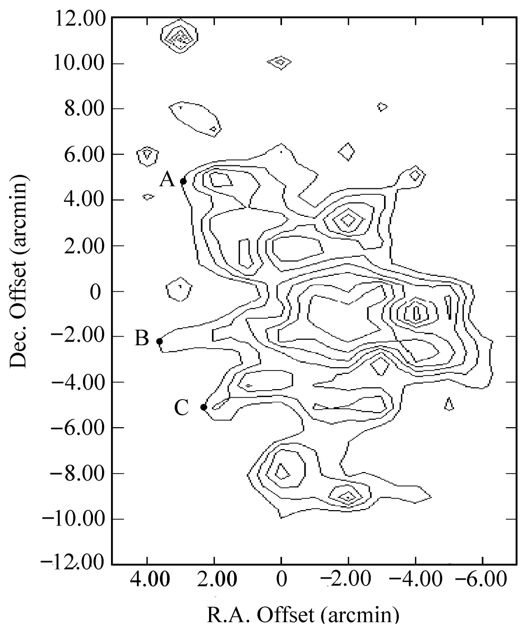

Fig. 2 Contour map of the integrated intensity, $\int T_A{}^* \, dv$, of $C^{18}O$ ($J = 1 - 0$) emission in the core of L134. Contour levels range from 0.50 to 1.10 K km s^{-1}in steps of 0.12 K km s^{-1}. The size of the mapped region is about $13'(\alpha) \times 25'(\delta)$ with a grid spacing of 1′. The central position (0.0′, 0.0′) of the map is biased to the east and leaves the bulk of the cloud in its west. The three points A, B, and C are at the periphery of the $C^{18}O$ cloud confined by the contour line of $\int T_A{}^* \, dv = 0.5$ K km s^{-1}.

Figure 2 shows the contour map of the integrated intensity ($\int T_A * dv$) of $C^{18}O$ ($J = 1 - 0$) emission in the dark cloud core of L134. The contour levels are in steps of 0.12 K km s^{-1} ranging from 0.50 to 1.10 K km s^{-1}. In the map several local peaks, for instance at the positions ($-4.0'$, $-1.0'$) and ($-2.0'$, $3.0'$), can be identified. The position ($0.0'$, $0.0'$) is not near the $C^{18}O$ cloud center, and it is rather biased to the east. The nominal center position coordinates of $\alpha = 15^h51^m15^s$, $\delta = -4^\circ\ 35'00''$ (1950) for HI map (van der Werf et al. 1989) and $\alpha = 15^h51^m00^s$, $\delta = -4^\circ\ 30'00''$ (1950) for OH map (Mattila et al. 1979) are not much different from ours, while their origins are basically surrounded by the bulk of HI and OH clouds, respectively. However, in the ^{13}CO map (Minn et al. 1996) the center position of L134, $\alpha = 15^h51^m30^s$, $\delta = -4^\circ\ 42'00''$ (1950), is at the south-east of the map, and the bulk of ^{13}CO molecules is not distributed around it, but covers the $C^{18}O$ cloud we have obtained. In comparison with the visual extinction data of L134 derived by Cernicharo & Bachiller (1984), the position ($0.0'$, $0.0'$) of our $C^{18}O$ map is inside the extinction distribution, and the bulk of the $C^{18}O$ cloud except its northern part is distributed inside the boundary labeled by the visual distinction of 6.9 mag (fig. 6 in Minn et al. 1996). On the other hand, to compare our map with the interstellar blue extinction, A_B, in the L134 region derived by Mattila et al. (1979), the $C^{18}O$ cloud is entirely included in the dust distribution of L134.

4 DISCUSSION AND CONCLUSIONS

The study of OH observations of the dark cloud L134 (Mattila et al. 1979) showed that, in the L134 region, the distributions of the antenna temperatures and the integrated intensities of OH lines correlate remarkably well with that of interstellar blue extinction, A_B. Moreover, the OH distribution agrees very well both in the position of maximum intensity and in size with the H_2CO distribution, and both distributions agree with the opaque core ($A_B \geq 9.7$ mag) of the dust cloud, according to Mattila et al. (1979), which also claimed a good correlation between the column density of ^{13}CO molecules and that of OH molecules. Furthermore, Minn et al. (1996) plotted a combined contour map of integrated intensities of ^{13}CO ($J = 1 - 0$) and 6 cm H_2CO lines together with the visual extinction distribution, which shows that ^{13}CO, H_2CO, and dust have quite a similar geometry and peak positions. Thus it may be concluded that the mass distributions of OH, ^{13}CO, and H_2CO are well correlated with that of dust. The size of the $C^{18}O$ cloud is about $9.5'(\alpha) \times 16'(\delta)$ as confined by the contour of $\int T_A^* dV = 0.5$ K km s^{-1}, and is nearly included in the ^{13}CO map. The ^{13}CO map has a southern extension beyond the $C^{18}O$ confines, however, which is reasonable because $C^{18}O$ molecules trace the smaller but denser portion of a cloud than ^{13}CO molecules do. To study the $C^{18}O$ gas depletion onto dust grains, we compare the $C^{18}O$ map we have obtained with the dust distributions, and find that the blue extinction map (fig. 3 in Mattila et al. 1979) is large enough to include the $C^{18}O$ cloud, and the visual extinction map (fig. 6 in Minn et al. 1996) basically does the same except that the northern part of the $C^{18}O$ cloud extends slightly beyond the contour of 6.9 mag in the visual extinction data, but probably the northern part is still in the area of extinction less than 6.9 mag. For a more detailed study we take three points at the periphery of the $C^{18}O$ map: A ($3.0'$, $4.7'$) at north-east, B ($3.6'$, $-2.2'$) at east, and C ($2.3'$, $-5.1'$) at south-east, then superpose the $C^{18}O$ map on the A_B map of Mattila et al. (1979) shown in fig. 3, in which the dashed frame indicates the area of the $C^{18}O$ distribution. We can see that in the blue extinction map only the point A sits on the contour level between 1.0 and 9.7 mag, which is approximately taken to be 4.7 mag, and the points B and C together with the bulk of the $C^{18}O$ cloud are inside or very close to the $A_B \geq 9.7$ mag contour. Now we estimate the degree of the $C^{18}O$ depletion onto dust. According to the definition of the depletion factor η, the factor, which is an average along the line of sight (Kramer et al. 1999), can be expressed as

$$\eta = (N(\mathrm{C}^{18}\mathrm{O})/A_V)_C/(N_m(\mathrm{C}^{18}\mathrm{O})/A_V)\,, \tag{1}$$

where $(N(\mathrm{C}^{18}\mathrm{O})/\mathrm{A}_V)_C = 1.6\times10^{14}$ cm^{-2} mag^{-1} is the canonical abundance ratio for the $\mathrm{C}^{18}\mathrm{O}$ column density N ($\mathrm{C}^{18}\mathrm{O}$) and the visual extinction $A_{V,}$ and $N_m(\mathrm{C}^{18}\mathrm{O})$ is determined on the basis of LVG (large velocity gradient) model in the case of Kramer et al. (1999), but we simply use the column density derived from $\int T_R^* dV$ and A_V from the A_B map, assuming that the normal interstellar reddening law is valid, i.e., $A_B = 4.0E(B-V)$ for the color excess $E(B-V)$. The $\mathrm{C}^{18}\mathrm{O}$ column density is expressed as (Sato et al. 1994)

$$N(\mathrm{C}^{18}\mathrm{O}) = 2.24\times10^{14} \int T_R^* dV/(1-\exp(-5.27/T_{\mathrm{ex}}))\ \mathrm{cm}^{-2}\,, \tag{2}$$

where $T_{\mathrm{ex}} = 12\,\mathrm{K}$ (Mahoney et al. 1976; Tucker et al. 1976) in L134 and $\int T_R^* dV$ is in units of K km s^{-1}. Note that the bulk of the $\mathrm{C}^{18}\mathrm{O}$ map is covered by the area confined by $A_B \geq 9.7$ mag contour as mentioned above; in other words nearly all the contour lines of the $\mathrm{C}^{18}\mathrm{O}$ map are inside the region confined by the blue extinction $A_B = 9.7$ mag, when the minimum A_B is adopted. Assuming the canonical ratio is valid in our case, the calculated depletion factors η are listed in Table 1.

Table 1 Calculated Depletion Factors η

Position*	$\int T_A^* dv$ (K km s^{-1})	A_B (mag)	$N_m(\mathrm{C}^{18}\mathrm{O})/A_V$ (10^{14} cm $^{-2}$ mag^{-1})	η
A	0.5	4.7	1.47	1.09
B, C	0.5	9.7	0.71	2.25
Λ_1	0.5	9.7	0.71	2.25
Λ_2	0.62	9.7	0.88	1.82
Λ_3	0.74	9.7	1.05	1.52
Λ_4	0.86	9.7	1.22	1.31
Λ_5	0.98	9.7	1.39	1.15
Λ_6	1.10	9.7	1.56	1.02

*: a) A, B, and C are at the positions (3.0′, 4.7′), (3.6′, –2.2′), and (2.3′, –5.1′), respectively.
b) Λ_s, its subscript s from 1 to 6, denotes the positions located on the contour lines of the $\mathrm{C}^{18}\mathrm{O}$ map, which are labeled by the values of $\int T_{\mathrm{A}}$* dv and are in the area confined by extinction of ≥ 9.7 mag.

If we assume that the measured antenna temperatures in other positions in L134 have the same relative error as that at the position $(0.0', 0.0')$ mentioned in Sect. 2, and all the parameters in Eqs. (1) and (2) remain constant except T_{A}^*, the relative error of the calculated η is then 0.16. Apparently it is a lower limit. Nevertheless, the depletion factors in the central core are probably higher than the values we have calculated at least for two reasons. One is that there is only a minimum $A_B = 9.7$ mag available in the blue extinction map of the L134 core, and in reality the blue extinction reaches as high as a limiting magnitude of ~ 23 mag in the photograph taken by an optical telescope for this region (Mattila 1979). The other is that our observations measure both undepleted and depleted areas along the line of sight. Willacy et al. (1998) have estimated how much of the $\mathrm{C}^{18}\mathrm{O}$ emission comes from the dense dust core (the central core) and how much from the outer regions, and found that the depletion is much higher in the central core than calculated, although their estimate is not quite certain. The main contribution of the $C^{18}O$ emission arises from outside of the central core, where the visual extinction is lower, so the depletion in the central core could be larger, and so the calculated η in Table 1 are most likely underestimated. Additionally, if we took for $N_m(C^{18}O)$ the LVG value as given in Kramer et al. (fig. 8c in Kramer et al. 1999), which is lower than what we take, the depletion factor would also be greater. It is also likely that some gas depletion exists beyond the $C^{18}O$ cloud boundary, which is defined by $\int T_A^* dv = 0.5$ K km s^{-1}, if the extinction there is large enough, for example, in the region to the south-east of the dashed frame in Fig. 3, where the extinction is still 9.7 mag or more. To compare the blue extinction distribution (Mattila et al. 1979) with the visual extinction data of L134 derived by Cernicharo & Bachiller (1984), we find they are not much different, and we expect to reach the same conclusion that the CO depletion onto dust occurs in the bulk of the $C^{18}O$ cloud, when we apply the latter's data to this depletion analysis. There is no direct evidence as yet for star formation in L134, which appears to be gravitationally unstable, as suggested by Mattila et al. (1979). Therefore the verge of the core collapse will not be visible in CO and many other molecules because of the gas depletion onto dust. Reasonably, measurement of infrared emission by dust grains seems a more reliable tool to investigate such regions.

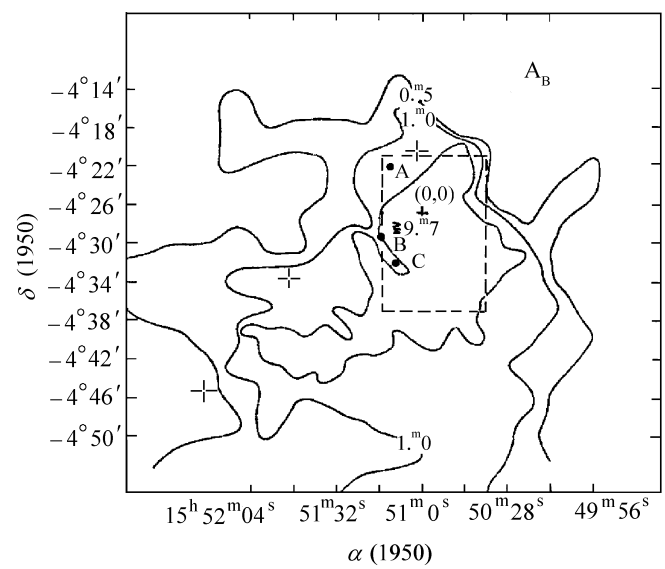

Fig. 3 Region of the $C^{18}O$ cloud indicated by the dashed frame superposed on the blue extinction distribution (Mattila et al. 1979). The points of A, B, and C in the $C^{18}O$ map are shown on the A_B map.

Acknowledgements We would like to thank all the staff at the Qinghai Station of Purple Mountain Observatory for their support and hospitality during the observing session. Also we want to thank Drs. Jiang-Tao Su and Xing-Ming Bao at the National Astronomical Observatories for part of the map making. Finally we are grateful to the anonymous referee for his/her significant suggestions.

References

Brooks J. W., Sinclair M. W., Manefield G. A. et al., 1976, MNRAS, 177, 299

Cernicharo J., Bachiller R., 1984, A&AS, 58, 327

Goldsmith P. F., Langer W. D., 1978, ApJ, 222, 881

Kramer C., Alves J., Lada C. J. et al., 1999, A&A, 342, 257

Mahoney M. J., McCutcheon W. M., Shuter W. L. H., 1976, AJ, 81, 508

Mattila K., 1979, A&A, 78, 253

Mattila K., Winnberg A., Grasshoff M., 1979, A&A, 78, 275

Minn Y. K., Lee H. K., 1996, JKAS, 29, 75

Sato F., Mizuno A., Nagahama T., 1994, ApJ, 435, 279

Tucker K. D., Dickman R. L., Encrenaz P. J. et al., 1976, ApJ, 210, 679

van der Werf P., Goss W. M., Vanden Bout P. A., 1988, A&A, 201, 311

Willacy K., Langer W. D., Velusamy T., 1998, ApJ, 507, L171